GCEP award #51922:
A Novel Solid Oxide Flow Battery Utilizing H-C-O Chemistry

Investigators

Gareth Hughes, Graduate Researcher; David Kennouche, Graduate Researcher; Zhan Gao, Post-doctoral Researcher; Scott A Barnett, Professor, Materials Science and Engineering, Northwestern University

Chris Wendel, Graduate Researcher, Pejman Kazempoor, Post-doctoral Researcher, Robert Braun, Assistant Professor, Robert Kee, Professor, Mechanical Engineering, CSM

Abstract

This project centers on a novel device that stores energy electrochemically in tanks like a flow battery, while the materials and chemistry are more akin to those of a solid-oxide fuel cell – hence the name "Solid Oxide Flow Battery" (SOFB). The SOFB is well suited for grid-scale energy storage because the energy storage capacity can be increased by increasing tank storage capacity. The objective of the project is to carry out the fundamental studies of the materials, cells, stacks, and system designs needed to validate the device concept and provide the information needed for further development. One set of challenges for SOFB technology includes the development of cells that yield the desired performance at the desired operating temperature and pressure, and that can work without significant degradation over thousands of electrolysis/fuelcell cycles. Other challenges are to develop viable stack and system designs that can yield the predicted ideal round-trip efficiencies of ~ 80%.

In the third year of this project, good progress has been made on a number of fronts ranging from electrochemical cell fabrication, to cell testing under a range of conditions including pressurization, to system-level simulations. Briefly, novel materials and SOFBs developed in this program have been tested under conditions required for efficient energy storage, i.e., below 600^{o}C or under pressurization to ~ 10 atm. Results on cyclic testing of air electrodes and full cells show that degradation is eliminated for current density below ~ 0.8 A/cm^2. Pressurized testing of cell electrode materials is providing fundamental new information on their behavior versus pressure. The past year's efforts have focused on developing cell-level models for reversible SOFB operation and extending energy storage system studies to include technical evaluations of both large-scale and distributed-scale grid-energy storage. One highlight has been the development and analysis of a promising new system configuration, where a pressurized, intermediate-temperature SOFB is coupled with pressurized natural gas underground storage caverns, providing high round-trip efficiency along with large storage capacity and relatively low storage cost.

Introduction

The need for grid-scale electrical energy storage is becoming more acute as increasing amounts of intermittent renewable electrical sources come on line, making it increasingly difficult to match fluctuations in both supply and demand [1, 2]. Daily supply/demand cycles mean storage times of ~ 12 h, requiring the ability to store very large amounts of energy. Currently available methods generally fail to meet at least one of the main storage-technology criteria – cost, efficiency, storage capacity, durability, and widespread availability [1-4]. Hydroelectric water pumping and underground

compressed air storage are well established but limited to specific naturally-occurring geographic sites. Secondary batteries and ultracapacitors currently have limitations for storing large amounts of energy cost effectively. Flow batteries may provide more scalable storage, although electrolyte volume and cost scale with energy stored [5, 6]. Reversible fuel cells have received only limited consideration for energy storage – although they have potential for large-scale storage, round-trip efficiency is usually relatively low [7, 8].

This project aims to demonstrate and develop a novel "Solid Oxide Flow Battery" (SOFB) for large-scale energy storage. This unique device occupies a new space that has similarities to, but is quite distinct from, both solid oxide fuel cells and flow batteries. The devices are different than flow batteries since the storage fluids are very-low-cost gases rather than expensive liquid electrolytes, and the operating temperature is higher. They are also different than solid oxide fuel cells, as they operate reversibly rather than in one current direction, and at lower temperature and higher pressure.

Figure 1 shows a simplified schematic of the proposed SOFB energy storage system. The membrane-electrode assembly (MEA) is based upon ceramic components that are designed to operate at 600-750˚C. In solid-oxide fuel cell (SOFC) mode, electricity is produced (discharge) as the fuel flows from the "SOFC Fuel" tank through the MEA, with the exhaust collected in "SOEC Fuel" tank. In solid-oxide electrolysis cell (SOEC) mode, the flow reverses direction, with electricity stored chemically (charging) in the "SOFC Fuel" tank. Oxygen flows through the lower channel. Oxygen ions are transferred through a dense ceramic membrane within the MEA.

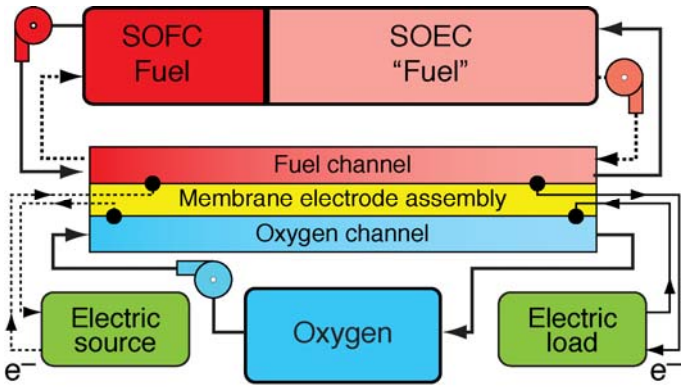

Figure 1. Simplified process flow diagram for the SOFB concept. Discharging is shown with solid lines and charging with dashed lines.

In conventional high-temperature H_2O or CO_2 electrolysis, relatively high electrolysis voltages are used to provide the input energy needed to compensate for the highly endothermic reactions. This ultimately leads to relatively low round-trip storage efficiency. Our SOFB concept is designed to overcome efficiency limitations by altering the products of electrolysis of H_2O-CO_2 mixtures. That is, by producing CH_4 in addition to H_2 and CO, the overall reaction becomes less endothermic, allowing lower electrolysis voltages and higher efficiency. In our proposed method, CH_4 production is increased by operating the SOFB with a C-H-O fuel-gas mixture at either (1) a relatively low temperature of $\approx$ 600^{o}C and 1 atm, or (2) an increased pressure of 3-15 atm and a more usual operating temperature of $\approx$ 750^{o}C. In a more recent embodiment, the cells operate

at $\approx$ 600°C and under pressurization of ~ 20 atm, which has the same advantages as the other modes but, in addition, it results in a very CH_4-rich product that can be stored in existing pressurized natural gas underground caverns.

With the above unique approach used to improve efficiency, the SOFB has the potential to meet the desired large-scale energy storage criteria and also has some unique advantages:

- High round-trip efficiency;
- Large amounts of energy can be stored over time scales of hours or days, limited only by the size of the storage tanks, and yet the SOFB system can also respond quickly;
- Reasonable cost: using current cost targets for solid oxide fuel cells and an energy storage time of 12 h yields a very desirable stack cost for energy storage of approximately $70/kWh;
- Solid electrolyte and tank leakage are minimal, yielding negligible energy loss during storage;
- The technology should have minimal environmental impact and uses mostly abundant and non-toxic materials of construction.
- SOFBs will integrate into the electrical network similar to other electrochemical storage devices; since energy is stored primarily as methane, they have the additional unique feature of allowing integration with the natural gas network;
- SOFB technology development will benefit substantially by leveraging prior/current development of solid oxide fuel cells, that has already advanced towards establishing good long-term stability, a route to low-cost large-scale manufacturing, and scale-up with > 100 kW demonstrations;

Given that no other widely available technology meets all the requirements, this innovative concept has the potential to be a game changer and play an important role in enabling extensive use of renewable energy. However, the technology will require substantial development from the state of the art in the closely related technology – solid oxide fuel cells. As noted above, SOFB requirements are significantly different than fuel cells, due to the unique operating conditions (low temperature and/or high pressure) and the need to work reliably upon many cycles between charge and discharge mode. This requires fundamental new cell materials development work, along with development of novel stack and system designs.

The research project aims to validate that the SOFB concept can yield high efficiency, and greatly extend current knowledge on solid oxide cell operation at high pressures and low temperatures. New cell materials, microstructures, and designs are being developed. State-of-the-art methods for observing materials evolution during accelerated testing are being employed to assess and improve long-term stability. The work benefits from synergies between innovative cell development, experimental evaluation, fundamental physically-based modeling at the cell and stack level, and system-level modeling including balance-of-plant performance. Achieving high efficiency while producing enough excess heat to offset thermal losses and maintain the stack operating temperature ultimately depends on combined cell/system optimization. Thus, cell/system modeling is employed to guide cell performance targets and materials development in a concurrent R&D engineering approach that is expected to accelerate technology development.

The research is intended to provide sufficient proof-of-concept data to justify further investment in larger-scale development and implementation; the next stage would be

development of a moderate-scale (~ kW) device. If expected targets are reached, the technology is anticipated to compete quite effectively against other storage technologies, providing strong motivation for commercial development.

Background

The field of energy storage using solid oxide cells continues to grow. This area, along with that in the broader field of solid oxide fuel cells, is important because it improves the science and technology background supporting the present work. Much of the recent work is on unidirectional cell operation, converting input renewable energy into chemical fuels. The group at Danish Technical University (Energy Conversion Department) continues to lead this field. The research group at Julich, Germany has also been active, in particular publishing two reports recently on the long-term stability of solid oxide cells under electrolysis and fuel cell modes.[9, 10] The main lab in the U.S. developing solid oxide electrolysis applications, Idaho National Labs, has been active in the past but currently has limited funding in this area.

Outside of our group, there has been relatively little work published related to the use of solid oxide cells for reversible electricity storage, but we are seeing increased activity and interest at scientific conferences.

Results

The results are divided into three main parts:

1) Development of solid oxide cells specifically designed for the energy storage application;

2) Testing of solid oxide cells under the pressurized and intermediate temperature conditions needed for efficient energy storage;

3) Thermodynamic calculations that suggest a storage option producing almost pure methane; and

4) Detailed and physically realistic system-level modeling based on measured cell characteristics to determine optimal operating conditions and to predict system characteristics including round-trip efficiency, storage capacity, *etc.*

1. Solid Oxide Cell Development

Two types of solid oxide cells with (La0.9Sr0.1)0.98(Ga0.8Mg0.2)O3-δ (LSGM) electrolyte, and bi-layer electrolyte consisting of Gd-doped Ceria (GDC) and Yttria-stabilized Zirconia (YSZ), have been further developed, improved, and tested. The latter cells are an important new development - when these are modified with improved cathodes and a thinner YSZ layer to reduce ohmic resistance, they will become important contenders for intermediate-temperature SOC storage devices. Finally, both types of cells are now made using tape casting, a major development because this method is widely used for large-scale manufacturing.

Cells With Thin LSGM Electrolytes

These cells are now made using tape casting yielding highly controlled layer thicknesses and microstructure. They consist of a (Sr,La)TiO_3 support, a Ni-impregnated LSGM anode functional layer, and thin dense LSGM electrolyte, and a (La,Sr)(Fe,Co)O_3-GDC composite cathode. The peak power density of 1.34 Wcm^{-2} is reached when the

operating temperature is 650°C, and 0.9 Wcm^{-2} at 600°C. These are already very good intermediate-temperature solid oxide cells (IT-SOCs), but we expect to further improve them in the future by utilizing an improved cathode material. The anode functional layer already has a very low resistance after an optimization study that we carried out. The optimal anode contained 30 wt% Ni and had a porosity level achieved by using 30 wt% of graphite pore former in the anode functional layer formulation.

Ceria-Zirconia Bi-Layer Electrolyte Cells

Solid oxide fuel cells (SOFCs) with bi-layer Zirconia/Ceria electrolytes have been studied extensively because of their great potential for producing high power density at reduced operating temperature, important for reducing cost and thereby allowing broader SOFC commercialization. The bi-layer electrolytes are designed to take advantage of the high oxygen ion conductivity of Ceria, the low electronic conductivity of Zirconia, and the low reactivity of Ceria with high-performance cathodes. However, Zirconia/Ceria processing has proven problematic due to interdiffusion during high temperature co-firing, or ceria layer porosity after two-step firing. We have developed a new method for bi-layer co-firing at a reduced temperature of 1250°C, ~ 150°C lower than the usual sintering temperature, achieved using Fe_2O_3 as a sintering aid. This novel process enables high power density SOFCs by producing: (1) low-resistance $Y_{0.16}Zr_{0.92}O_{2-\delta}$ (YSZ)/$Gd_{0.1}Ce_{0.9}O_{1.95}$ (GDC) electrolytes that also yield high open-circuit voltage, (2) dense GDC layers that prevent reactions between highly-active $La_{0.6}Sr_{0.4}Fe_{0.8}Co_{0.2}O_3$ (LSFC) cathode materials and YSZ, and (3) Ni-YSZ anodes with high electrochemical activity due to fine-scale microstructure with high TPB densities.

In order to demonstrate the advantages of the present process, cells fabricated at 1250°C were compared directly with otherwise identical cells fired at 1400°C. The 1250-fired cell yielded power density of 1.48 Wcm^{-2} at 0.7 V at 800°C, substantially higher than the 1400-fired cell - 0.94 Wcm^{-2} at 0.7 V. The OCV values of the 1250-fired cells, which had Fe in the YSZ layer, were quite similar to that of the Fe-free 1400-fired cells, indicating that any electronic conductivity caused by Fe doping is negligible. These results correlated directly with a change in the ceria/zirconia interface, as observed by transmission electron microscopy (TEM), with the 1250°C firing giving a much smaller interdiffusion zone.

The reduced firing temperature also improved anode performance. The reasons for this were explored using three-dimensional tomography.**[11, 12]** The tomographic data show that decreasing the firing temperature from 1400 to 1250°C yielded decreased mean particle sizes – from 0.66 to 0.51 μm for Ni and from 0.61 to 0.45 μm for YSZ, respectively. The decreased temperature yielded higher active three-phase boundary (TPB) density – an increase from 3.0 to 7.2 μm^{-2} – that is explained by the smaller particle sizes.**[13-15]** The higher active TPB density explains the lower resistance associated with the anode electrochemical process. The 1250-fired cell also had a slightly higher pore volume fraction, presumably due to reduced sintering at the lower firing temperature, that also leads to a decrease in pore tortuosity. Both these changes increase gas diffusivity and thereby decrease concentration polarization.

Optimization of the bi-layer electrolyte was carried out with different Fe doping levels added to the YSZ and GDC layers. It was found that the best quality interface was obtained for YSZ with 1 mol.% Fe_2O_3 and GDC with 2 mol.% Fe_2O_3. At other doped

levels, the interfaces had a high density of voids, apparently due to poor shrinkage matching during the sintering process. The cells with optimized electrolytes yielded maximum power densities > 2 Wcm^{-2} at 800°C, 1.73Wcm^{-2} at 750°C, 1.23 Wcm^{-2} at 700°C, 0.75 Wcm^{-2} at 650°C respectively. These cells shows some of the highest electrolysis current densities ever reported. For example, the electrolysis voltage was as low as 1.06V at 1Acm^{-2} at 800°C, with an overpotential of only 0.13V at 1Acm^{-2}. Life testing under different current densities showed there was no apparent degradation at 0.5 Acm^{-2}, and slight degradation at 0.75Acm^{-2}, where the degradation rate was ~ 3.3%/kh.

2. Solid Oxide Cell Testing

High-Pressure Electrochemical Testing

In order to be able to accurately model solid oxide cells operated under pressurized conditions, we have carried out measurements of electrode performance under pressurized conditions. (Note that electrolyte resistance does not typically vary with pressure.) The work so far has focused on oxygen electrodes, which typically provide the main limitation on intermediate-temperature cell performance.

Impedance spectra taken for a (La,Sr)(Fe,Co)O_3- Gd-doped ceria (LSCF-GDC) composite electrode at 700°C at various oxygen partial pressures P_{O2} show obvious changes with increasing P_{O2} – a shift to higher frequency and a decrease in the magnitude of the impedance. At the lowest pressure, there appear to be peaks at 10 Hz and at 1 Hz. The peak at ~ 1 Hz is probably due to gas diffusion; it follows the expected trend that it decreases rapidly as P_{O2} increases. The peak at ~ 10 Hz increases in frequency and decreases in size with increasing P_{O2}. A plot of the total impedance versus P_{O2}, shows that the decrease in impedance has a slope of ~ - 0.25 ($R_P \propto P_{O2}^{-0.25}$), a dependence often seen due to a charge transfer limited process. Overall, the reduction in electrode resistance on going from 0.2 atm O_2 (air) to 10 atm O_2 is substantial, from 0.17 to 0.11 Ω cm^2. This would lead to a significant improvement in overall cell performance.

Another material system investigated was the LSM-YSZ ($(La_{0.8}Sr_{0.2})_{0.98}MnO_3$ - $Zr_{0.84}Y_{0.16}O_2$) composite electrode that is widely used in SOFCs. Unlike the LSCF-GDC electrode described above, the polarization resistance decreased at a constant slope throughout the entire measured pressure range. The slope was similar, however, ~ - 0.3, again probably signifying that the oxygen reduction reaction was limited mainly by a charge transfer process. There was little indication of the low frequency gas diffusion loss at low P_{O2}, or the new process at high frequency. This may be due in part to the higher overall resistance – if the charge transfer process has a high resistance, it is less likely that other processes will become important. There is another possible explanation for not seeing the high frequency process, which was tentatively attributed to solid-solid interfaces in the above arguments. In particular, in LSM-YSZ the charge transfer process occurs at three-phase boundaries, with the oxygen ions going directly into the YSZ phase, and then ultimately into the YSZ electrolyte. Thus, there are no additional interfaces for oxygen ions to cross, unlike LSCF-GDC where oxygen exchange occurs at the LSCF surfaces followed by transport from the LSCF into the GDC.

Additional experiments are underway to isolate the changes in air-electrodes using the dual-atmosphere rig designed for the high-pressure testing setup at atmospheric pressures. The rig has been designed to seal a SOFC button cell with different controlled atmospheres on either side, allowing new experiments to be conducted where each

electrode experiences a different oxygen partial pressure. This has allowed the observation of oxygen gradient induced voltages and will allow more detailed examination of the processes occurring within the electrodes at different points of the SOFB cycle.

SOFB Durability Testing

Our previous reports have detailed measurements to determine whether electrodes can work without substantial degradation under the reversing current conditions required for the energy storage application. Surprisingly, solid oxide cells have not previously been studied in this way, so these are perhaps the first published reports on cycling operation. Our previous report detailed measurements of LSM-YSZ electrodes, arguably the most important ones in terms of durability. Here, we have extended these measurements to a second important oxygen electrode system, LSCF-GDC. Furthermore, we have explored the role of overpotential and current density on degradation.

The behavior of a LSCF-GDC / GDC / LSCF-GDC symmetric cell was tested in the same test setup and under similar conditions as those used in prior LSM-YSZ cycling life tests. Thus, the two electrodes can be compared directly. The test was completed using a lower operating temperature of 700C, lower than the 800C value used for LSM-YSZ, since it has a characteristically lower operating temperature. The test was run at a current density of 1.5A/cm^2 for 0.5 h in each current direction, i.e., a reversing current cycle period of 1 hour. A direct comparison of the LSCF-GDC and LSM-YSZ shows shows a steady total resistance increase for the LSCF-GDC cell, but at a lower rate than the LSM-YSZ cell. The main difference was in the ohmic resistance, which increased much less for LSCF-GDC. On the other hand, the polarization resistances of both cells showed a similar degradation rate.

The reduced degradation of the GDC electrolyte in the LSCF-GDC cells can be attributed to its slightly increased electronic conductivity over YSZ. The mechanism explained by Virkar et. al. [16], formation of oxygen gas bubbles in the electrolyte leading to eventual electrolyte/electrode delamination, is predicted to have reduced effectiveness when the electrolyte material has a slight electronic conductivity, as seen in GDC.

Studies on LSM-YSZ were continued, based on prior results that showed no degradation at a current density of 0.5 A cm^{-2}, but rapid degradation at 1.5 A cm^{-2}. Thus, it was important to determine what is the maximum current density that yields acceptable degradation rates – typically ~ 0.5 %/kh. Using an identically processed LSM-YSZ cell as reported previously, the current was incrementally increased every ~150 hours from 0.5A/cm^2 to 1.5A/cm^2. The start of degradation in both ohmic and polarization resistance can be seen, but they start at different points. The polarization resistance starts increasing at 900mA/cm^2, but the ohmic resistance does not start to increase until 1200mA/cm^2.

3. Thermodynamic Calculations

Further investigations exploring different possible operating modes of SOFB electricity storage system have been carried out. ThermoCalc software was used to predict the equilibrium gas compositions and thermo-neutral voltages for a new condition: intermediate temperature and elevated pressure. (Previously, we considered either intermediate temperature or elevated pressure.) The goal here is to produce high

methane content output from the cell, which can be stored directly in existing pressurized natural gas underground caverns. A brief summary of the results is provided here.

A range of C/H ratios, temperatures, and pressures were studied to determine the effect of each on the methane content in the output fuel, as well as investigating how changing the end points of the system would change the energy output. The parameters were guided by the systems analysis, detailed below, which show that the highest round-trip efficiency can be expected when the SOFB stack is at a pressure midway between ambient and the underground cavern pressure, ~ 150 atm. A typical result for the gas constitution versus operating temperature, for a pressure of 20 atm, a C/H ratio of 1/5.5, for electrolysis carried out to an output oxygen content of 8% O_2, shows that the methane content increases with decreasing temperature, reaching > 50% below 600°C. There is some further improvement with further temperature decrease, with the methane content increasing from ~ 50 to ~ 57% from 600°C to 400°C. Note that for an operating temperature of 500°C, the methane content is nearly >78% (balance H_2) after the H_2O is condensed out of the product upon cooling to ambient temperature for storage. This product gas could go directly into existing natural gas storage. Also note that the thermo-neutral voltage for these conditions is ~ 1.0 V, such that electrolysis can be done at relatively low overpotentials that are consistent with high efficiency and low degradation.

4. Results from Physically Based Cell and Systems Modeling

Physically-based cell modeling plays a central role in the SOFB research effort, spanning from fundamental electrochemistry to stack performance. There are three main objectives associated with high fidelity cell modeling. One objective of this task is to develop and validate the fundamental theory and modeling framework of reversible solid oxide cells. Another primary objective is to extend fuel-cell models to include electrolysis operation and to represent new materials and cell architectures. The system level modeling, design, and analysis tasks seek to elucidate attractive system architectures that enable the high efficiency SOFB cell-stack performance to be retained. Additionally, system modeling interjects critical feedback into the SOFB materials/cell/stack research process by providing a holistic viewpoint that is cognizant of grid energy storage requirements and balance-of-plant constraints.

The past year's efforts have focused on developing cell-level models for reversible SOFB operation and extending energy storage system studies to include technical evaluations of both large-scale and distributed-scale grid-energy storage. In the following, reversible cell modeling is first summarized followed by systems-level trade studies on key SOFB operating parameters related to temperature, pressure, and reactant composition. System configuration analyses and a summary of efficiency improvements are also given.

Physically based Cell Modeling[*]

The reversible solid oxide cell (SOC) model employed here builds upon our previous efforts used separately for SOFC and SOEC studies.[17-19] As a noticeable advancement to our prior efforts, the latest model employs a more general formulation of the electrochemical model of the cell which helps to provide a more robust simulation of rSOC behavior in both fuel cell and electrolyzing modes. In this manner, the model can

[*] See publication #2 for further details.

easily switch from one mode to another mode by changing the sign of the electrical current (" –" for SOEC and "+" for SOFC modes). A detailed description of the modeling approach and formulation is beyond the scope of this annual report, but details can be found in our recent publication.[17] Of primary importance is the improvement in electrochemical modeling, especially with regard to activation polarization modeling and in extending single-cell models to be representative of stack performance through incorporation of an additional ohmic (contact) resistance between cell layers.

Since the main focus of the cell modeling effort is on the prediction of reversible operation of a cell-stack, the model was calibrated and validated in both modes of operation using a series of experimental data for a planar Ni/YSZ-supported SOCs of 5×5 cm with an active electrode area of 4×4 cm.[17, 18] The cell consists of a 10-15 µm thick Ni/YSZ cermet electrode supported by a ~300 µm thick porous Ni/YSZ layer, a 10-15 µm thick YSZ electrolyte, and 15-20 µm thick strontium-doped lanthanum manganite composite LSM/YSZ electrodes. The cell is sandwiched between the gas distributor components, which are contacted with a gold foil at the side of the LSM/YSZ electrode and a nickel foil at the side of the Ni/YSZ electrode. The experimental tests were performed at 750, 800, and 850 C with pure oxygen (20 L/h) passing over the sweep gas electrode and gas-mixture (i.e. CO_2, H_2O, H_2, CO, CH_4) or H_2/H_2O mixtures (25 L/h) passing over the fuel electrode. The cell is in a cross-flow configuration. Accordingly, this section first calibrates the model parameters for a reversible cell and then reveals its validity when the operating conditions change.

Model calibration seeks to extract fitting parameters for the Butler-Volmer terms in the activation polarization formulation in the electrochemical cell model. Accordingly, once calibration is achieved for a reversible cell, validation can proceed using different experimental operating conditions. In the following, three different sets of experimental data were employed to fit model parameters such that the electrochemical cell model properly represents the performance data as shown in Figure 17. Figure 17 illustrates that the calibrated model fits nearly perfectly with the experimental data.

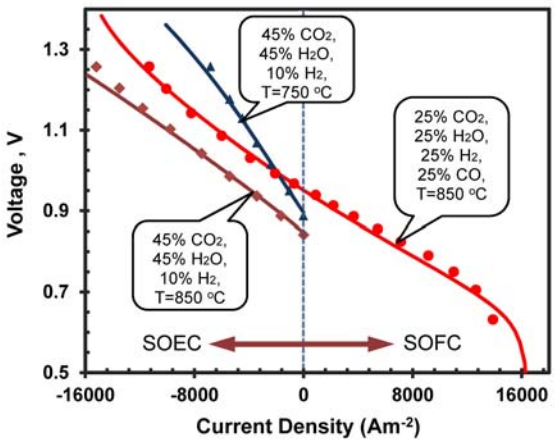

Figure 17. rSOC model calibration result

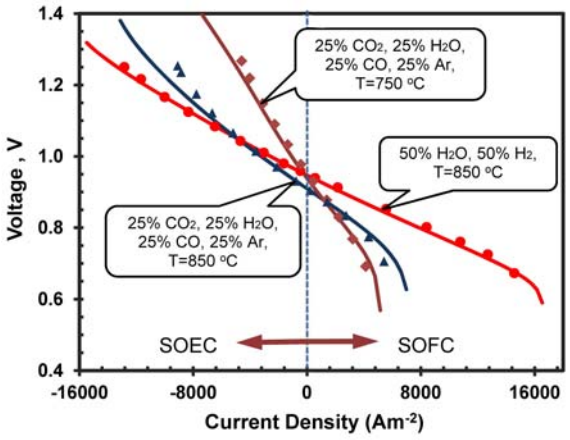

Figure 18. rSOC model validation result

By fixing the parameters determined from the model calibration effort, additional experimental results from the same cell have been considered for model validation. Figure 18 illustrates three examples of these cases. As can be seen, the model accurately simulates the rSOC behavior as the inlet gas composition and temperature deviate from

the values used in the calibration study. The maximum error observed between the experimental and numerical data is about 5% at current density ~9000 A/m^2 for 25% CO_2, 25% H_2O, 25% CO, 25% Ar gas mixture at 850^{o}C.

Our previous system modeling results have shown that operating cell temperature, pressure, fuel flow rate (or utilization), and fuel composition are key parameters for achieving SOFB systems with high round-trip efficiency. Thus, we have further explored the effects of these parameters through model predictive simulations at the cell level.

Effect of temperature on the rSOC voltage-current characteristic

The V-J characteristic of rSOCs strongly depends on the cell operating temperature as demonstrated in Figs. 17 and 18 (more polarization results when the cell temperature is decreased from 850 ^{o}C to 750 ^{o}C). Figs. 19 and 20 show a comprehensive analysis of the cell electrochemical losses at 850 ^{o}C and 750 ^{o}C for the base case. The polarization losses shown in these figures are the average values of the losses along the channel length. Comparing the two figures (Figs. 19 and 20), it is clear that both the magnitude and the distribution of the cell losses (at each current density) are significantly altered by changes in the operating temperature. At 850 ^{o}C, the total ohmic (i.e., ohmic plus contact losses) and oxidant electrode (or sweep gas electrode) activation polarizations contribute the most to the overall cell losses, followed by the fuel electrode (FE) activation and concentration losses, respectively. Note that the concentration polarization shown in these figures is the total cell concentration loss; although it is mostly affected by the polarization in the fuel electrode. With the exception of the ohmic loss, which follows a nearly linear trend, the other losses exhibit a non-linear behavior as the current density increases. This non-linearity is related to the variation of the gas mixture concentrations, as well as the cell temperature along the channel length. As shown in Figure 19, the FE and sweep gas electrode (SGE) activation losses are relatively lower in the SOFC mode than the SOEC mode which is related to the gas component concentrations and the considered symmetry factors. Figure 19 also illustrates that the total cell losses in each operating mode are approximately equal (i.e., symmetric) at 850°C.

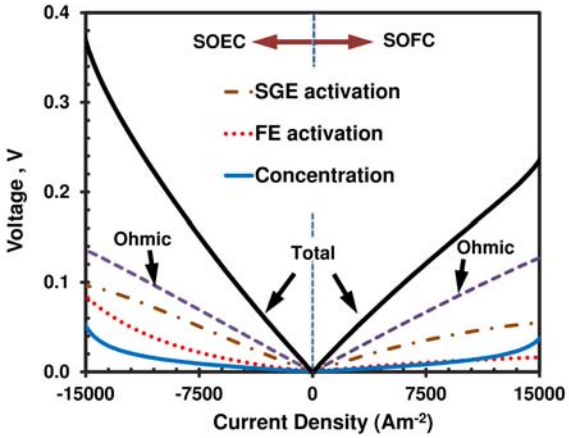

Figure 19. Break down of polarisation losses versus cell current density at 850^{o}C

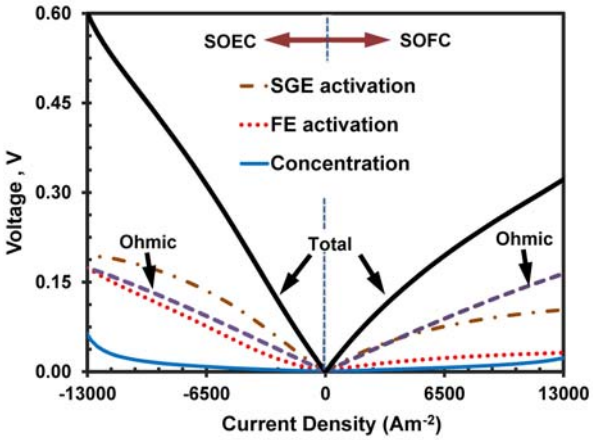

Figure 20. Break down of polarisation losses versus cell current density at 750^{o}C

Figure 20 shows the variation of the cell polarizations when the inlet feed gas temperatures vary between 850^{o}C to 750^{o}C. By reducing the operating temperature, the

activation polarization in both electrodes is increased significantly due to lower activity of the cell catalyst and surface reactions. It seems that the activation losses in the SOFC mode are less affected by the operating temperature than in SOEC mode. Decreasing the inlet gas temperature also significantly promotes the cell ohmic loss. However, as widely reported in the extant literature, this is to be expected given that the electronic and ionic conductivity of the ceramic materials used in rSOCs are strongly temperature dependent. In spite of the previous observation at 850 ^{o}C, a significant difference between the cell total losses at both operating mode can be seen at 750 ^{o}C.

The operating temperature not only alters the cell performance; the thermoneutral voltage also changes with temperature. The thermoneutral voltage generally is lower at low temperatures. However, it depends strongly on the reaction directions. For the above cases, the thermoneutral voltage decreases from 1.371 V to 1.340 V when the feed gas temperature changes from 850 ^{o}C to 750 ^{o}C. The thermoneutral voltage is higher at lower temperatures in some cases due to the WGS reaction direction.

Effect of the feedstock gas composition

The model calibration and validation cases presented above have shown that the feed gas composition noticeably affects the V-J characteristic curve. From our previous investigation on SOECs, it is concluded that electrochemical models constructed based on only the H_2 and H_2O electrochemical reactions (neglecting the CO and CO_2 electrochemical reactions) is more accurate at low and moderate CO_2/ CO inlet gas flow rates; although it is very hard to establish a criteria for the exact range. Considering this limitation, the FE gas composition is varied from H_2O/H_2 to a gas-mixture (i.e. CO_2, H_2O, H_2, CO, CH_4) in order to see how the cell V-J characteristic curve and the thermoneutral voltage vary as a function of the gas mixture. The effect of CH_4 through the methanation reaction is presented shortly.

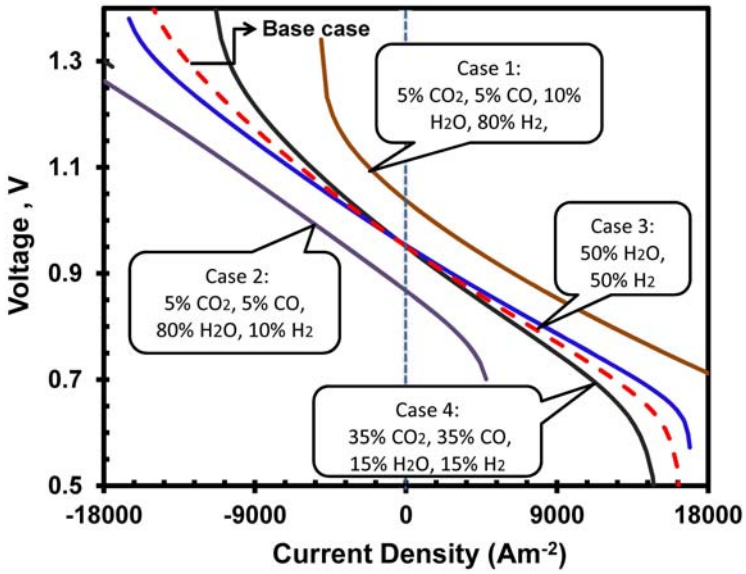

Figure 21. V-j characteristic curve at 850^{o}C with different feedstock gas composition

Figure 21 shows the V-J characteristic curves for four more mixtures shown beside the base case V-J curve (keeping the flow rates constant). Case 1 with the high H_2 mole

fraction shows an example of a favorable feedstock gas composition for SOFC mode. Due to the high concentration of the H_2, the Nernst potential for this case is relatively higher than the other cases. Although the SOC demonstrates favorable performance in the fuel cell mode, it experiences quite high polarization in the electrolyzing mode causing a limiting current density near 6000 Am^{-2}. As shown in Case 2, one can add more water into the inlet gas mixture in order to decrease the cell polarization during the electrolyzing mode. However, the cell performance in fuel cell mode will rapidly fall off with this condition. Case 3 shows an example of the cell operation with a 50% H_2-50% H_2O mixture as the feed gas into the FE electrode. In this condition, the V-J curve is located nearly evenly between the Case 1 and Case 2 curves and it is very close to the base case result. Since the cell losses (especially activation) are relatively high in CO_2/CO electrolyzing and fuel cell modes, the similar performance observed between Case 3 and the base case shows that when the concentrations of steam and hydrogen in the feedstock are sufficiently high, the main pathway for conversion of CO_2/CO gases is via rWGS/WGS reactions. Case 4 shows the V-J curve when the flow rate of CO_2/CO is relatively higher than the base case. In this condition, the cell polarization remains similar to the base case and Case 3 curves, especially at low current density (~6000 Am^{-2}). However, as the current density increases more deviation can be observed due to higher activation and concentration losses.

The thermoneutral voltage, which is a key parameter for SOEC operation, also changes slightly with the feed gas composition and temperature. In general, the variation of thermoneutral voltage shows that adding more CO and H_2O into the feed gas mixture decreases V_{tn} to values close to those observed for steam electrolyzing since it promotes the exothermic WGS reaction (more heat can be generated inside the cell in this condition). Conversely, increasing the mole fraction of CO_2 reverses the direction of the WGS reaction. Thus, the cell needs more heat due to endothermic nature of the rWGS reaction and consequently V_{tn} is increased in this condition.

Note that the main purpose of the electrolyzing mode is to convert the inlet gas to a storable fuel. As mentioned above, adding more CO and H_2O gases promotes CO_2 and H_2 production rates, decreasing the amount of the fuel produced during the SOEC mode by changing CO to CO_2 (noted that H_2 produced here can also be generated through the electrochemical reaction)

Methanation and pressurized operation

There is little reported experimental work on pressurized rSOC operation. As the cell pressure increases, the potential for the gas leakage, cell degradation, and other related losses is also increased which can make it challenging to produce reliable experimental data. These losses in addition to the pressurized test setup itself can affect and alter the cell performance. The Northwestern University effort on pressurized cell testing and operation will support these modeling efforts further. But at this time, without enough supporting test data in the following we only illustrate the qualitative behavior of a cell under pressurized operation and compare them with what experimental data is available in the literature. While the results presented here do not show the exact behavior observed in the experimental data given in Ref. [20], they clearly show the effect of the pressurized operation on both the cell kinetic reactions and gas species mass diffusion.

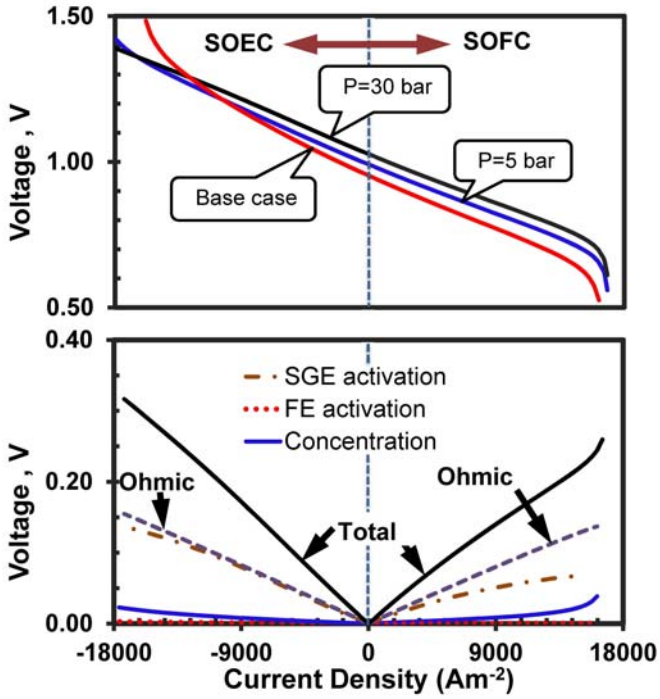

Figure 22. V-J characteristic curve and break-down of the cell polarizations for pressurized operation

Pressurized operation has two distinct effects on the cell performance. On the one hand, it enhances the electrochemical performance of the cell with increasing the Nernst potential and decreasing the losses associated with the activation and concentration polarizations. On the other hand, pressurized operation promotes the methanation reaction in the SOEC mode. Figure 22 demonstrates the V-J characteristic curve for the base case at three different pressures (1, 5, and 30 bar). The inlet feed gas temperatures are fixed at 850^{o}C for these cases. The break-down of the cell losses at 30 bar is also presented in the same figure which can be easily compared with the previous data for the base case at 1 bar (presented in Figure 19).

In addition to affecting the Nernst potential, pressurized operation also significantly reduces the cell kinetic losses and enhances the charge-transfer reaction kinetics by increasing adsorption rates and the surface coverage occupied by adsorbents. Comparing the break-down of the cell losses at 1 bar (Figure 16) and 30 bar (Figure 22), It can be seen that the activation losses, especially in the FE electrode, decrease considerably with increasing the pressure. Note that the formulations employed here for calculating the cell activation polarizations were originally developed for near atmospheric pressure conditions and their accuracy for pressurized operation is not yet validated. Although the V-J curves (at high pressure) have the same qualitative shape as experimental data presented in Ref. [20], more experimental and numerical activities are still needed to evaluate the cell activation losses at high pressure.

The low FE activation loss observed at 30 bar comes mainly from increased partial pressures of the gas species which is reflected in the Butler-Volmer formulation of this loss term (see Kazempoor and Braun [17]). As mentioned above, increasing the operating

pressure also enhances the transport of the reactant and product gases effectively shifting the limiting current density to higher values.

Pressurized operation does not have any direct effect on the cell total ohmic losses as it is a function of the cell temperature. However, as shown in Figure 22, the total cell ohmic loss in the electrolyzing mode is also reduced (compared to the data presented in Figure 19). Increasing the pressure implicitly changes the cell thermal behavior by promoting the endothermic methanation reaction. As a result, the cell temperature at each current density is relatively higher if the methanation reaction occurs inside the fuel channels. Generally, increasing the pressure and decreasing the temperature are two conditions favorable for formation of methane. The outlet mole fraction of CH_4 at various pressure and temperature is presented in Figure 23. As shown, the outlet mole fraction of CH_4 can even reach up to 28% at 30 bar and 750°C.

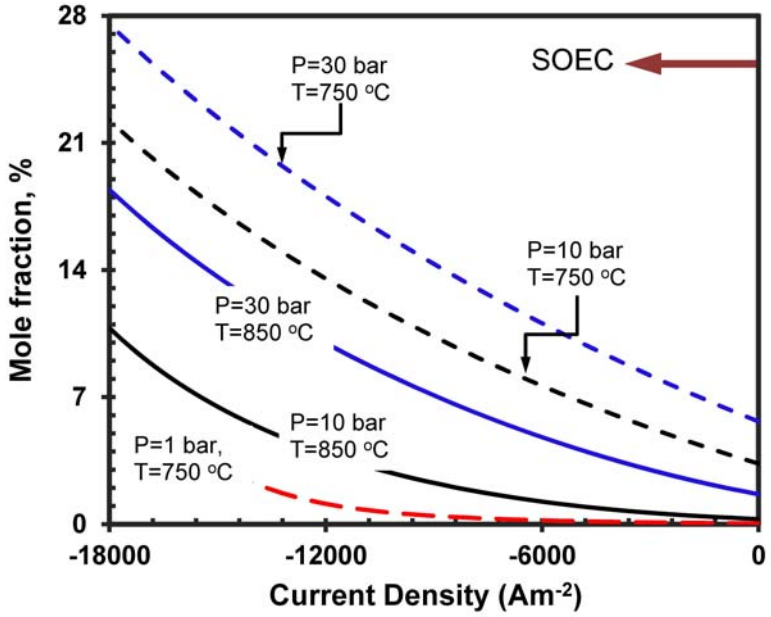

Figure 23. Outlet mole fraction of CH_4 at different pressures and temperatures

The combined effect of the above phenomena inside the rSOCs increases the overall performance of the cell in both pressurized operating modes. Note that, although in SOECs the Nernst potential increases at high pressure, the amount decreased from the cell losses due to pressurized operation (as described above) are more valuable than the increase in V_{tn}. As can be seen in Figure 22, after a certain current density (9000 Am^{-2} at 5 bar and 11600 Am^{-2} at 30 bar) the SOEC voltage and consequently SOEC power consumption ($=I \times V_{op}$) is lower at high pressures than the atmospheric condition.

Cell modeling summary

Extending the previous year's cell modeling efforts, we have developed a detailed channel-level interface charge transfer model for predicting reversible SOC electrochemical and thermal performance. The model was calibrated and validated versus experimental data. The calibration parameters were the activation and ohmic loss parameters. It has been observed that the model, when calibrated based on these parameters, can readily simulate the cell behavior and is valid when the cell operating

conditions deviate from the calibration cases. The model was then employed to investigate the effect of some key parameters necessary for the system study. The results from the parameter study enable the following conclusions to be drawn:

The SGE activation polarization and the ohmic resistances are generally the main contributors to the cell losses. However, the FE activation polarization can be relatively higher than other cell losses depending on the feedstock fuel flow rate and gas composition.

The total electrochemical losses of the cell can be significantly different in each operating mode depending on the operating conditions of the cell.

Decreasing the cell temperature slightly decreases V_{tn} (depending on the gas composition and WGS reaction direction). However, operating at low temperature increases the rSOC electrochemical losses. Decreasing the operating temperature also promotes the methanation reaction which is favorable for achieving thermoneutral electrolysis operation. Thus, it is generally more favorable to work at lower temperatures if there are not any significant differences between the cell performance at high and low temperatures.

It is observed that the practical way to decrease V_{tn} is to increase the pressure. Pressurized operation enhances the endothermic methanation reaction. With increasing the rate of methanation, the cell thermoneutral voltage can even be lower than V_{Nernst}, meaning the SOC operates in a heat generating mode in this condition.

Pressurized operation also has a significant effect on the cell thermal behavior and methanation.

System Modeling, Design, and Analysis

The following parametric studies consider the effect of rSOC stack temperature and pressure on system efficiency. These two parameters are significant because of their impact on stack thermal management, including the kinetic and thermodynamic effect on methane formation and steam-methane reforming. System operation is also impacted, for example, by the stack temperature influence on heat exchanger preheating and recuperation duties, and the stack pressure influence on compressor and turbine power consumption and generation.

System level modeling is employed to determine whether the theoretically high efficiency of rSOCs can be retained in a practical operating system and also to determine suitable system configurations and operating conditions that enable high-efficiency performance. Figure 24 shows the system concept being evaluated in the present effort. Unlike the GCEP team's system studies in 2012, we have considered separate water storage in this study, which is representative of a more practical system. In each mode of operation the reactant species, either from the "fuel" or "exhaust" tank, are expanded, preheated, and mixed with steam evaporated from a separate water storage tank before entering the stack. The reactants are converted to products in the rSOC stack with either consumption or generation of dc electric power. Finally, the product species from the stack are cooled to condense out any H_2O before compression and additional cooling for tank storage. Liquid water is stored separately such that evaporation, condensation, and additional pumping hardware are required. This configuration shows that much of the balance-of-plant (BOP) hardware can be utilized in both modes of operation, which is important for reducing system capital cost.

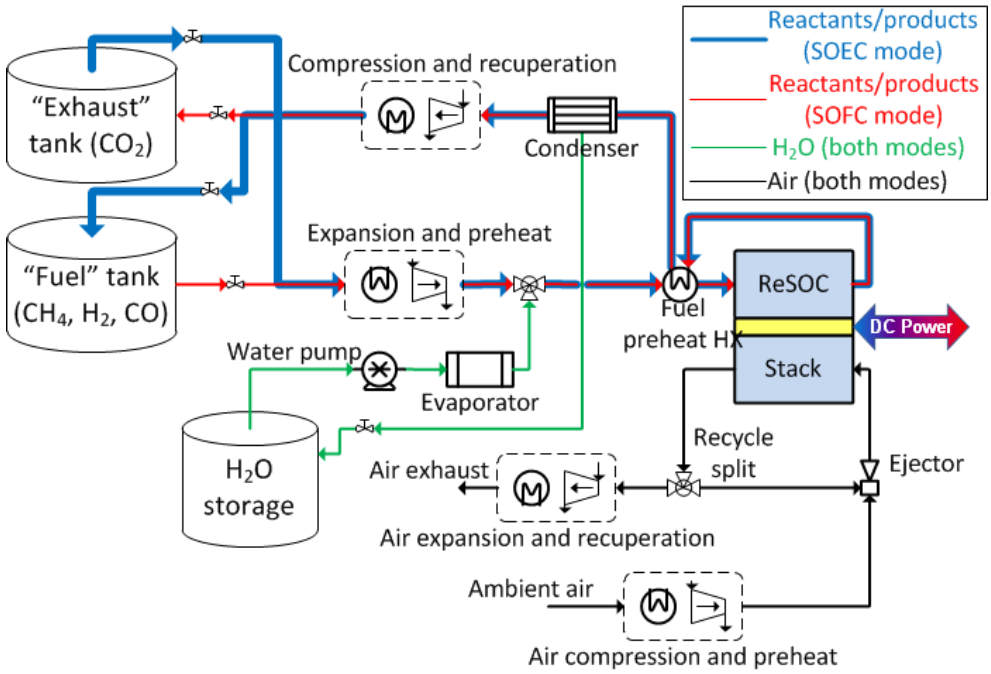

Figure 24. Energy storage system schematic

Additional BOP components are needed to preheat and compress air to the required stack inlet conditions and then to recuperate thermal and mechanical energy from the exhausted air after it is utilized in the stack. Furthermore, an ejector is employed to recycle some of the air flow exiting the stack to reduce the cost and power load of the BOP components with a slight penalty to stack efficiency.

The storage function of this system may assume a variety of configurations depending on the scale of application. For example, lower capacity distributed applications may economically employ pressurized tanks for storage of gaseous species while large capacity grid-scale applications may more economically utilize underground caverns such as has been done with natural gas and compressed air. A study on compressed air energy storage systems noted that above ground tanks are economically favorable compared to underground caverns up to sizes of around 40,000 m^3, above which the capital investment in developing an underground storage cavern is justified.[21] Furthermore, the use of fixed versus variable volume storage components will have considerable impact on dynamic operation. Specific storage configurations will not be considered at this point because under steady-state conditions the storage tanks are simply considered as sources and sinks.

Many BOP components must be thermally integrated in this system including pre-heat and recuperative heat exchangers, condenser, and evaporator; however, specific configurations of these thermal components are not declared at present. Rather, duty requirements are used to ensure the energetic feasibility of operation with a pinch temperature of >15°C and no violations of the 2nd Law.

System operating considerations

The selected current density and fuel composition are important model parameters that depend on the stack temperature and pressure. It is generally desirable to operate with high concentrations of carbonaceous species (i.e., low hydrogen-to-carbon ratio), for

example, using methane (CH_4) for stack and system thermal management. However, at the high operating temperatures (>550°C) of rSOC devices, carbon containing reactant gases can deposit coke on electrode surfaces, thereby reducing performance. Thus, the thermodynamic carbon deposition limit is considered to select reactant compositions that are expected to mitigate coke formation. Note that the system concept depicted in Figure 24 includes two gas compositions associated with the "fuel" and "exhaust" storage tanks, however it is not immediately clear which compositions are most suitable. Furthermore, because this is a closed system the reactant compositions are not determined by a feedstock input, such as natural gas in an SOFC power system or some ratio of steam and CO_2 in a co-electrolysis process. Instead, the gas occupying the "exhaust" tank is produced during SOFC mode where its composition is established from the SOFC stack operating conditions including temperature, pressure, and fuel utilization. Similarly, the composition of the gas in the "fuel" tank is established from the fuel channel product stream when the system is operated in SOEC mode at its respective operating conditions.

The two compositions are conveniently depicted on the C-H-O ternary diagram as shown in Figure 25. They have equivalent hydrogen-to-carbon ratios, but the oxygen content changes with the addition of oxygen during SOFC mode and removal of oxygen during SOEC mode. The possible compositions are bounded by the fully oxidized region and carbon deposition region. Solid carbon deposition causes irreversible damage in rSOCs (i.e., catalyst poisoning, increased mass transport resistance in the gas diffusion electrode, etc.) and its formation depends on many factors including temperature, pressure, composition, and current density. The thermodynamic carbon deposition boundary, however, is a function of temperature and pressure alone. Selection of viable gas compositions must mitigate carbon deposition, ensure sufficient methane for thermal management, and allow high fuel energy density for increased energy storage capacity. Thus, it is desirable to operate with a highly carbonaceous composition (i.e. low hydrogen-to-carbon ratio) that does not exceed the carbon deposition boundary.

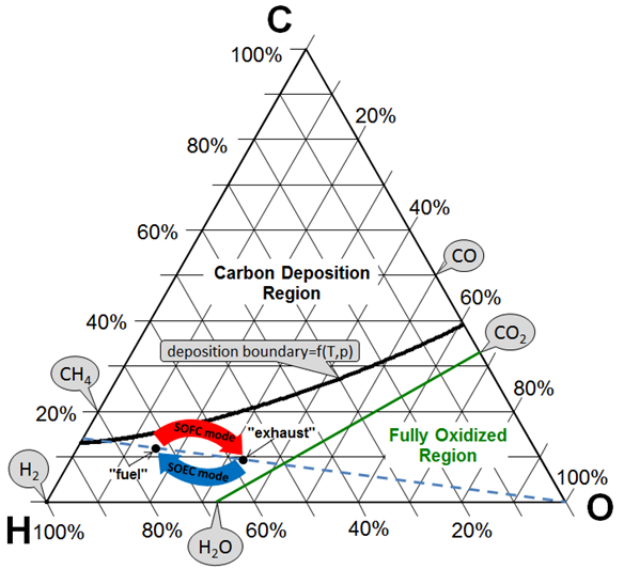

Figure 25. C-H-O ternary diagram depicting relevant species and possible "fuel" and "exhaust" reactant compositions

While the reactant composition must be set to mitigate coke formation, the current density is set such that enough waste heat is generated by the stack to meet the heating load of system BOP including preheating and steam evaporation processes. The waste heat generated within the cell stack due to resistive losses is a nonlinear function of the operating current density. However, waste heat is a direct result of stack inefficiencies, and operating the stack efficiently enough to maintain high roundtrip efficiency while also generating enough waste heat for gas processing is a challenge. In many stationary energy storage applications, high system efficiency is valued over high power density (i.e. high current density), although the balance between these performance parameters requires also considering economic impact. High system efficiency is achieved when both modes are operated at low current density, although thermal requirements must also be considered in determining a minimum current density.

Practically, the minimum current density is determined based on the thermal requirements in SOEC mode because a large quantity of steam must be generated and the electrochemical reduction reactions are endothermic. These endothermic processes are offset by heat generated in the stack from both methanation of generated fuel species and resistive heating associated with stack polarizations. If, for example, less heat is generated from the methanation reaction because of the selected fuel constituents or stack conditions (T, p), then a greater operating current density is required to provide the needed thermal energy. The 'discharging' (SOFC) mode is exothermic for all but very low current densities.

Selecting the current density in each mode of operation also requires considering the operating durations. For example, if the charge duration is twice as long as the discharge duration, then the discharge current density must be twice as large as the charging current density to return the system to its original state of charge. For our present effort, the charge and discharge duration are assumed to be equal, such that the current density is equal in both modes and is set to the minimum value that allows exothermic 'charging' (SOEC) mode.

System Modeling Results

The following parametric studies consider the effect of rSOC stack temperature and pressure on system efficiency. These two parameters are significant because of their impact on stack thermal management, including the kinetic and thermodynamic effect on methane formation and steam-methane reforming. System operation is also impacted, for example, by the stack temperature influence on heat exchanger preheating and recuperation duties, and the stack pressure influence on compressor and turbine power consumption and generation.

The effect of stack pressure

The operating pressure of the rSOC stack has a significant impact on the system efficiency. Importantly, stack pressure also affects the minimum current density required for exothermic charging, and the reactant composition which is expected to mitigate carbon deposition. Figure 26 shows the fuel composition in terms of the molar hydrogen-to-carbon (H/C) ratio and average stack current density as a function of rSOC operating pressure at a fixed average stack temperature of 650°C and storage pressure of 160 bar. A plot of the minimum H/C ratio needed to avoid carbon deposition shows that increasing

stack operating pressure enables higher concentrations of carbonaceous species in the "fuel" and "exhaust" compositions as predicted by the carbon deposition boundary.

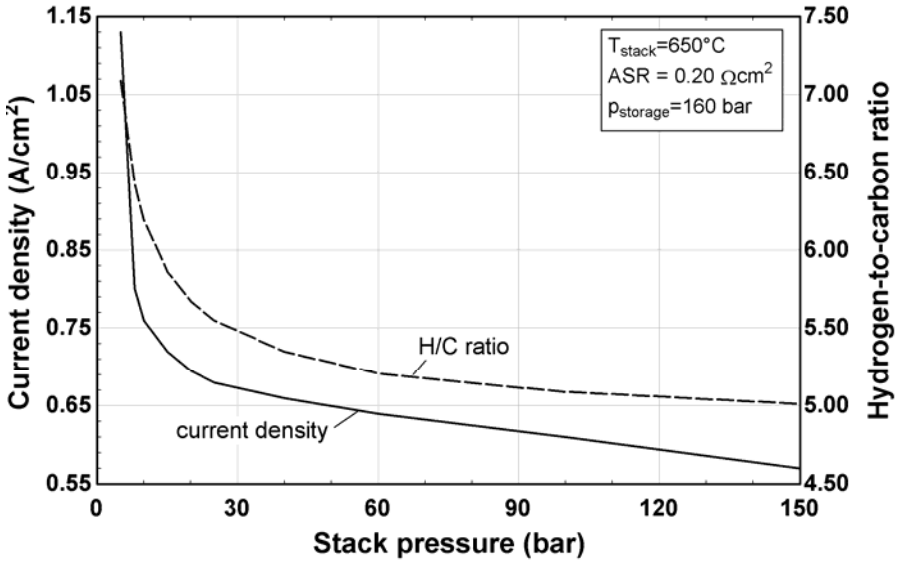

Figure 26. Current density and hydrogen-to-carbon ratio vs. stack pressure [22]

A certain amount of stack waste heat is essential to meet the heating load of system balance-of-plant including preheating and steam evaporation. As the rSOC stack pressure increases, more heat is generated from the methanation reaction in 'charging' (SOEC) mode; therefore less heat is required from stack inefficiency (i.e. resistive heating) and a lower current density is needed. Figure 26 shows the current density as a function of stack pressure, where the current density is relatively low at high pressure and increases sharply at lower pressure to overcome a heating deficit caused by lower conversion of the exothermic methanation reaction. There are two primary reasons for higher conversion of the methanation reaction at higher pressure: (1) the H/C ratio of the fuel composition decreases, approaching closer to the stoichiometric ratio for methane (i.e. H/C=4), and (2) increased kinetics of the methanation reaction.

The optimum roundtrip system efficiency is achieved based on a trade-off between stack efficiency and auxiliary power. Figure 27 illustrates that the roundtrip stack efficiency increases with increased stack pressure because the current density required for exothermic SOEC mode operation decreases (See also Figure 26). However, the increased stack efficiency is counterbalanced by increased auxiliary power consumption at high stack pressure.

The right-axis in Figure 27 shows the net auxiliary power generated in each mode as a fraction of the stack electric power where negative values are attributed to the auxiliary components consuming net power. At lower stack pressure, the SOFC mode auxiliary components produce net power because the turbine expansion of air exhausted from the stack produces more power than is required to compress air to the stack operating pressure. Yet, the benefit of net energy generation from the auxiliary components is overcome by a rapid decline in stack efficiency at low stack pressure. The competing trends of stack efficiency and auxiliary power result in an optimal system efficiency of 72.5% at a stack pressure of about 20 bar. The reason the SOFC mode auxiliary power

generation increases with decreased stack pressure is that the air does not need to be compressed to as great a pressure and the exhausted air from the stack can be expanded at higher temperatures while still performing the required heating processes.

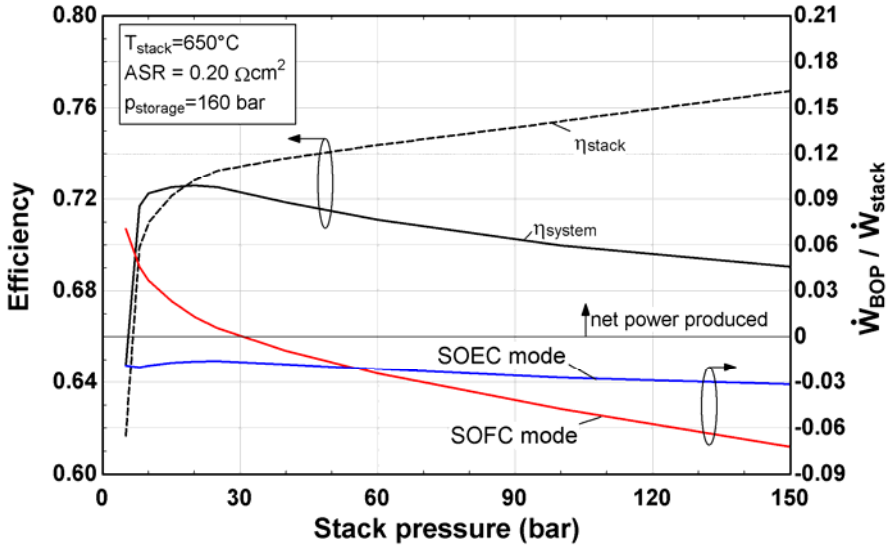

Figure 27. Stack and system efficiency (left) and BOP power relative to stack power (right) vs. stack pressure [22]

It is an important result that the system efficiency is significantly influenced by the system BOP because the desirable operating conditions expected from only analysis of the rSOC stack differ from the operating conditions that achieve optimal system efficiency. Furthermore, the optimal system configuration must, in addition to efficiency, also consider cost, dynamic operation and control, and a different configuration may achieve optimal efficiency at a different set of operating conditions.

Stack temperature parametric results

Reversible solid oxide cell materials and stack research has led to the possibility for highly efficient cell stacks that operate at temperatures considerably lower than the typical high temperature cells (>800°C), including intermediate (650-800°C) and low temperature (450-650°C) ranges. Thus, for a novel system design, it is important to consider the performance impact of the stack operating temperature to aid in selecting a suitable rSOC material set.

The average stack temperature impacts roundtrip efficiency; however, as shown in the previous parametric study, much of this impact can be understood by considering the effect of stack operating temperature on the hydrogen-to-carbon ratio of the reactant gas mixture and average operating current density. Figure 28 illustrates how the current density and H/C ratio of the reactant mixtures vary with changes in average stack temperature. The H/C ratio is set based on the thermodynamic carbon deposition limit and increases with increased temperature. The required average current density to meet process thermal loads decreases with increasing stack temperature in the low temperature range primarily because the exhaust airflow used to supply heat to the evaporator in 'charging' (SOEC) mode exits the stack at a lower temperature, therefore necessitating

more heat generation in the stack to satisfy pinch-point temperatures. A minimum current density is reached at an average stack temperature of about 680°C. At higher temperatures the required current density increases because more waste heat is required from the stack at higher temperatures where the exothermic methanation reaction has lower equilibrium conversion.

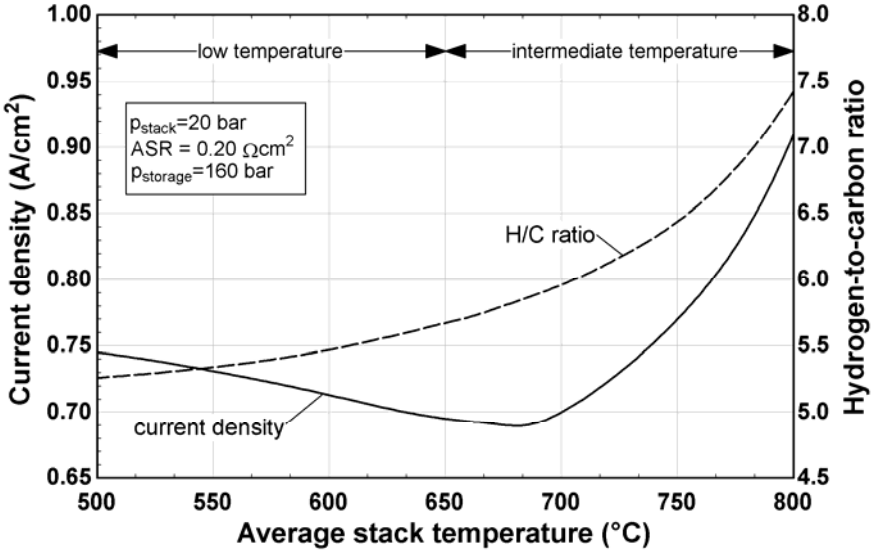

Figure. 28. Current density and hydrogen-to-carbon ratio vs. stack temperature [22]

Figure 29 shows the stack and system roundtrip efficiencies as a function of average stack temperature. System efficiency is maximized at an intermediate operating temperature of about 680°C and is primarily influenced by the stack efficiency and discharge mode auxiliary power. The stack efficiency increases slightly with increased stack temperature at lower temperatures and then drops off sharply at temperatures above 700°C in accordance with the increased current density (see also Figure 28). The SOFC (discharge) mode BOP power shifts from consuming net power at lower temperatures to producing net power at higher temperatures. The net auxiliary power generation in SOFC mode increases with increased average stack temperature primarily because the excess air exhausted from the stack is at a higher temperature such that more power is generated from expanding it to ambient pressure. Additionally, one conclusion from these results indicates that low temperature cell operation (<650°C) is not necessarily a materials requirement for rSOC energy storage systems configured in this way, so long as the stack pressure is sufficiently high.

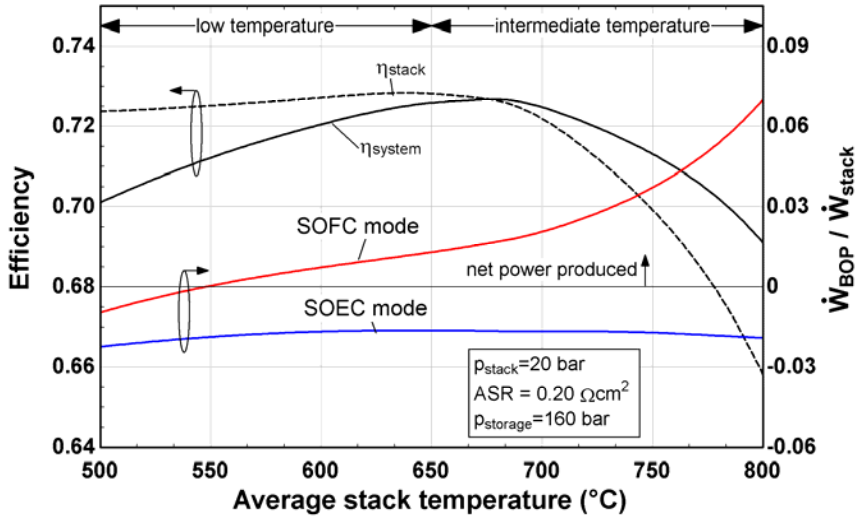

Figure 29. Stack and system efficiency (left) and BOP power relative to stack power (right) vs. stack temperature [22]

System modeling summary

The past year's system modeling efforts have analyzed the SOFB system efficiency over a range of stack temperatures and pressures. By implementing a thermal management strategy using carbonaceous reaction chemistry it was shown that >70% roundtrip storage efficiencies can be achieved when water is managed and stored separately within the system (as opposed to 'storing' gaseous H_2O). Steady-state system modeling results indicate that system efficiency is maximized at intermediate rSOC stack operating conditions of about 680°C and 20 bar based on the trade-off between stack efficiency and BOP behavior. The auxiliary power generation has a significant effect on system efficiency, and it is important to note that this impact could change for alternate system configurations, potentially shifting or eliminating the optimal efficiency points. It is promising, however, that the initial results imply optimal behavior at intermediate operating conditions such that extreme operation (i.e. low temperature, high pressure) are not necessarily required for efficient energy storage. Finally, because of the wealth of system configurations possible for implementation of such a system, further modeling work must consider alternate system configurations and additional performance metrics such as capital cost and levelized cost which require higher fidelity system modeling.

The system modeling results given thus far are representative of large-scale SOFB energy storage systems that could be deployed for GWh capacity levels that may be required to achieve high penetration of renewable resources, such as wind and solar. As noted in the Introduction to this report, large amounts of energy can be stored over time scales of hours or days or even seasons, limited only by the size of the storage tanks. Thus, it is quite possible to imagine the use of underground cavern storage that serves as the 'storage tanks'. Figure 30 depicts such a system concept with the 'ReSOC' meaning reversible solid oxide cell. The system modeling results given above are applicable to this system because the cavern storage is envisioned at 160 bar, and the study results are independent of size of the storage.

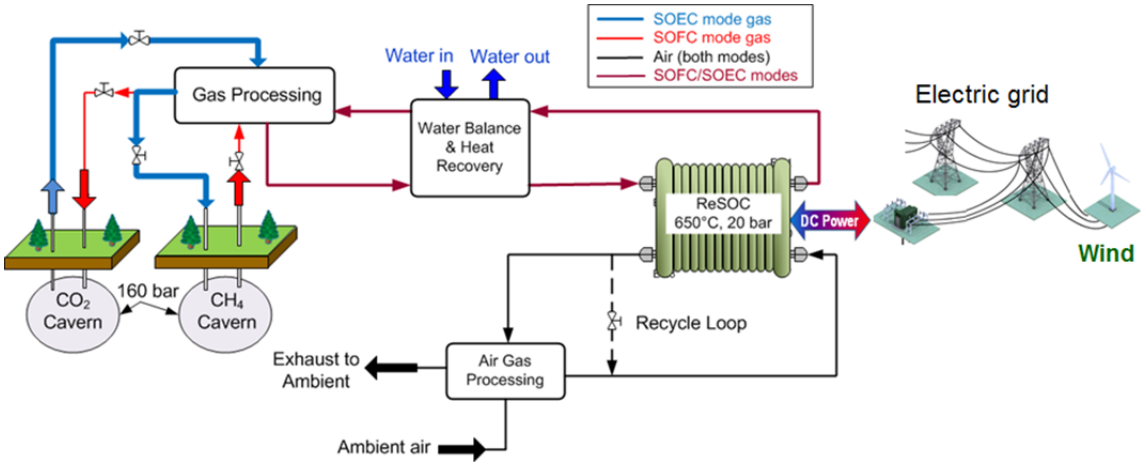

Figure 30. System concept for large-scale GWh energy storage using SOFB technology

Progress

Renewable electricity sources such as wind and solar are the primary alternative to fossil-fueled generation, and hence are critical for greenhouse gas reduction. However, the intermittent nature of these sources poses a formidable barrier to their adoption at significant fractions of our total electricity production. Thus, efficient and low-cost grid-scale energy storage must be a key part of plans to reduce greenhouse gas emissions. Although the technology being developed in this project is new and needs validation at many levels, it is still important given that currently available storage methods generally fail to meet at least one of the main storage-technology criteria – cost, efficiency, storage capacity, durability, and widespread availability. The results obtained in the past year have filled in many important details regarding materials, SOFB device characteristics, and system design. Particularly important are the observations that practical reduced-temperature SOCs are available and appear to be robust, reversing cell operation does not cause degradation, and that degradation is eliminated for the moderate current densities that are consistent with high efficiency. The system results are particularly compelling: the model is based on realistic cell data and cost information, and shows that a pressurized intermediate-temperature SOFB system connected to pressurized natural-gas underground storage caverns can provide grid-scale storage for times well beyond days with high round-trip efficiencies and at costs that are better than other electrochemical devices and competitive with pumped hydro storage. Overall, the results continue to show exciting promise for this technology.

Future Plans

Stability studies of cells designed for high pressure operation will focus more on the fuel electrode, as the oxygen electrode has already been characterized. Durability testing will also be extended to pressurized conditions, an area where there is little or no data in the literature. There will also be more emphasis on durability testing of full cells over the upcoming year. Exit-gas constitution measurements will be analyzed to reveal whether the fuel electrode has sufficient catalytic activity to produce a near-equilibrium product. The cell-level modeling capability will increasingly be used to assist in the quantitative interpretation of experimental cell-test results and help guide experimental lines of investigation.

Cell modeling will be extended to include pressurized operation and low temperature cell data from Northwestern. System modeling will proceed to establishing dynamic systems modeling for evaluating mode switching and system response capabilities. Steady-state modeling will continue with development of two optimized energy storage system design concepts at different scales: (1.) large-scale grid-energy storage (> 100 GWh), and (2.) distributed-scale electrical energy storage (~10 MWh). Electrical energy storage systems analysis will include economic analysis.

Publications and Patents

1. Kazempoor, P., and Braun, R.J., Model validation and performance analysis of regenerative solid oxide cells for energy storage: Electrolytic operation, Int J Hydrogen Energy (2014); 39:2669-84.
2. Kazempoor, P., and Braun, R.J., "Model validation and performance analysis of regenerative solid oxide cells for energy storage applications: Reversible operation," *Int. J. of Hydrogen Energy* 39:5955-5971 (2014).
3. Kazempoor, P., Wendel, C.H., and Braun, R.J., "Pressurized Regenerative Solid Oxide Cells for Electrical Energy Storage," *ECS Transactions*, 58(37): 45-54, (2014).
4. Kazempoor, P., and Braun, R.J.; "Performance Analysis of Solid Oxide Electrolysis Cells for Syngas Production," *ECS Transactions* 58(19): 43-53, (2014).
5. Wendel, C.H., Kazempoor, P., and Braun, R.J., "Operating conditions and system considerations for a reversible solid oxide cell system for electrical energy storage," *Proc. Of the 12th ASME Fuel Cell Science, Engineering and Technology Conference,* ESFuelCell 2014, June 29-July2, Boston, MA, (2014).
6. Gao, Z., Kennouche, D. & Barnett, S. A. Reduced-temperature firing of solid oxide fuel cells with zirconia/ceria bi-layer electrolytes. *Journal of Power Sources* **260**, 259-263, doi:10.1016/j.jpowsour.2014.03.025 (2014).
7. Gao, Z. & Barnett, S. A. Effects of Reduced Firing Temperature on Anode-Supported Solid Oxide Fuel Cells. *J. Electrochem. Soc.* **In press** (2014).
8. Miller, E. C., Gao, Z. & Barnett, S. A. Fabrication of Solid Oxide Fuel Cells with a Thin (La0.9Sr0.1)0.98(Ga0.8Mg0.2)O3-δElectrolyte on a Sr0.8La0.2TiO3Support. *Fuel Cells* **13**, 1060-1067, doi:10.1002/fuce.201300155 (2013).
9. Hughes, G. A., Yakal-Kremski, K. & Barnett, S. A. Life testing of LSM-YSZ composite electrodes under reversing-current operation. *Physical chemistry chemical physics : PCCP* **15**, 17257-17262, doi:10.1039/c3cp52973h (2013).
10. Gao, Z. & Barnett, S. A. Reduced-Temperature Firing of Anode-Supported Solid Oxide Fuel Cells. *Electrochemical Synthesis of Fuels 2* 58, 231-242, doi:Doi 10.1149/05802.0231ecst (2013).
11. U.S. Patent: Robert J Braun, Robert Kee, and Scott A Barnett, High efficiency, reversible flow battery system for energy storage US #8637197 B2 (Filed prior to the inception of the GCEP project)

12. U.S. Provisional Patent Application: Gao, Z., Miller, E., Barnett, S.A., Fabrication Of Solid Oxide Fuel Cells With A Thin (La0.9Sr0.1)0.98(Ga0.8Mg0.2)O(3-Delta) Electrolyte On A Sr0.8La0.2TiO3 Support, Serial No. 61/909,895 Filing Date: November 27, 2013
13. U.S. Provisional Patent Application: Gao, Z., Barnett, S.A., Anode-Supported Solid Oxide Fuel Cell Fabricated by Single-Step Cofiring, Serial Number: 61/897,583 Filing Date: October 30, 2013

References

[1] R. Dell, D. Rand, Journal of Power Sources, 100 (2001) 2-17.
[2] in: http://arpa-e.energy.gov/portals/0/Documents/ConferencesandEvents/Pastworkshops/Grid Scale Energy Storage/GS-Sum.pdf, Department of Energy, Seattle, 2009.
[3] J. Baker, Energy Policy, 36 (2008) 4368-4373.
[4] **http://www.electricitystorage.org/ESA/applications/**, (2009).
[5] M.H. Chakrabarti, R.A.W. Dryfe, E.P.L. Roberts, Electrochimica Acta, 52 (2007) 2189-2195.
[6] C. Ponce de León, A. Frías-Ferrer, J. González-García, D.A. Szánto, F.C. Walsh, Journal of Power Sources, 160 (2006) 716-732.
[7] W. Smith, Journal of Power Sources, 86 (2000) 74-83.
[8] F. Barbir, T. Molter, L. Dalton, International Journal of Hydrogen Energy, 30 (2005) 351-357.
[9] F. Tietz, D. Sebold, A. Brisse, J. Schefold, Journal of Power Sources, 223 (2013) 129-135.
[10] V.N. Nguyen, Q. Fang, U. Packbier, L. Blum, International Journal of Hydrogen Energy, 38 (2013) 4281-4290.
[11] J.S. Cronin, J.R. Wilson, S.A. Barnett, J. Power Sources, 196 (2011) 2640-2643.
[12]D. Kennouche, Y.C.K. Chen-Wiegart, J.S. Cronin, J. Wang, S.A. Barnett, J. Electrochem. Soc., 160 (2013) F1293-F1304.
[13] J.H. Lee, H. Moon, H.W. Lee, J. Kim, J.D. Kim, K.H. Yoon, Solid State Ionics, 148 (2002) 15-26.
[14] K.R. Lee, S.H. Choi, J. Kim, H.W. Lee, J.H. Lee, J. Power Sources, 140 (2005) 226-234.
[15] Y. Nishida, S. Itoh, Electrochim. Acta, 56 (2011) 2792-2800.
[16] A.V. Virkar, International Journal of Hydrogen Energy, 35 (2010) 9527-9543.
[17] P. Kazempoor, R.J. Braun, Int J Hydrogen Energy, 39 (2014) 2669-2684.
[18] P. Kazempoor, V. Dorer, F. Ommi, Fuel Cells, 10 (2010) 1074-1094.
[19] P. Kazempoor, C.H. Wendel, R.J. Braun, ECS Transactions, 58 (2014) 45-54.
[20] S.H. Jensen, X. Sun, S.D. Ebbesen, R. Knibbe, M. Mogensen, International Journal of Hydrogen Energy, 35 (2010) 9544-9549.
[21] T. Petersen, B. Elmegaard, A.S. Pedersen, Technical Report to the Danish Technological Institute, (2013).
[22] Wendel, C.H., Kazempoor, P., and Braun, R.J., "Operating conditions and system considerations for a reversible solid oxide cell system for electrical energy storage," *Proc. Of the 12th ASME Fuel Cell Science, Engineering and Technology Conference,* ESFuelCell 2014, June 29-July2, Boston, MA, (2014).

Contacts

Scott A Barnett:	s-barnett@northwestern.edu
Zhan Gao:	zhan.gao@northwestern.edu
Gareth Hughes:	g-hughes@u.northwestern.edu
David Kennouche:	DavidKennouche2011@u.northwestern.edu
Robert Kee:	rjkee@mines.edu
Rob Braun:	rbraun@mines.edu
Pejman Kazempoor:	pkazempo@mines.edu
Chris Wendel:	cwendel@mines.edu